

Study of UV Filters as an *in silico* (QSAR) Graduate Project

D. González-Arjona^{1,*}, G. López-Pérez¹, A. Gustavo González², M. M. Domínguez¹, W. H. Mulder³

¹Department of Physical Chemistry, Universidad de Sevilla, Sevilla, Spain

²Department of Analytical Chemistry, Universidad de Sevilla, Sevilla, Spain

³Department of Chemistry, University of the West Indies, Kingston, Jamaica

Abstract A simplified *in silico* QSAR study, involving more than 50 molecules that are commonly used as UV filters in sunscreens, is presented. Details of methodology are described and illustrated step by step and the use of available tools is demonstrated, including data set selection, generation of molecular structure files, selection of computational methods, assessment of the relative importance of molecular properties, generation of theoretical UV-Vis spectra and construction of a QSAR model. With the aim of introducing the QSAR methodology at undergraduate level, some simplifications have been made. Multiple Linear Regression (MLR) has been selected as a modeling strategy to correlate the molecular descriptors and the sunlight blocking effect. The full area under the UV-Vis spectrum has been used as a simple measure of the protection factor. Theoretical UV-Vis spectra have been generated by using the configuration interaction (CI) approximation. The ground state molecular geometry has been optimized by the semi-empirical ZINDO computational method. Inclusion of a solvent model in the optimization of molecular geometry to account for solvatochromic effects has not been considered. On the other hand, total number of rings, number of aromatic rings, molecular dipole moment and HOMO/LUMO energy gap, are considered to be significant parameters in the MRL model. The HOMO/LUMO energy gap is the variable of choice when optimized single linear regression analysis is carried out separately for each of the functional groups of the compounds. The great variety of tools and procedures used in building QSAR models has been found to provide ample scope for active involvement by the students, exposing them to a fairly broad array of modern methods in areas like drug discovery and toxicology.

Keywords QSAR, Sunscreens, UV-VIS absorption, Graduation projects

1. Introduction

More than half a century has passed since Hansch et al [1] laid the foundations of the modern methodology of “Quantitative Structure-Activity Relationships” (QSAR), initially building on the work of Polanyi and subsequently Hammett who introduced the concept of “Linear Free Energy Relationships” (LFERs), by correlating the chemical structure of the phenoxyacetic acids with their biological activity in plant growth. Since then, QSAR has evolved to a point where it provides reliable, statistically predictive models.

Designing a chemical compound that possesses certain properties is usually very complicated relative to the effort involved in synthesizing a particular molecular structure. Although it may be relatively easy to deduce a reaction mechanism from a knowledge of molecular structure, it is often far more difficult to predict its properties based on this

structure. Whereas the reactivity appears as an intrinsic characteristic of the molecule this is not necessarily true for physicochemical or biological properties. The peculiar properties and behavior of a compound depend on both its internal structure and the molecular environment in which it finds itself. The surroundings interact with the entire molecule and more strongly so with specific sites. However, unlike chemical reactions, these interactions are relatively weak and do not lead to the breaking or formation of chemical bonds. Therefore, the modeling needed to relate the structure and a particular activity quantitatively, QSAR, is not a trivial task.

The use of QSAR models for the screening of chemical/biological products is a matter of great interest in both the chemical and pharmaceutical industry, toxicology, medicine, environmental studies, etc. The QSAR modeling method appears as one of the most useful tools in the understanding and prediction of properties and effects of chemical/biological compounds in the areas of environment and health. This methodology constitutes an efficient and operative means of assessing chemical hazards. In addition, the use of QSAR offers other advantages, such as low cost, high degree of investment recovery and it may even reduce

* Corresponding author:

dgonza@us.es (D. González-Arjona)

Published online at <http://journal.sapub.org/jlce>

Copyright © 2017 Scientific & Academic Publishing. All Rights Reserved

the need for using animals in laboratory testing of new drugs. All these applications have attracted the growing interest from government agencies for *in silico* predictions [2, 3]. Clearly, QSAR modeling is a multidisciplinary subject, which combines aspects from computer science, chemistry, statistics (cheminformatics) and knowledge of disciplines, particularly toxicology, that explore the activity of chemicals as it relates to health and environment.

The mechanism underlying the protection by sunscreens is well known. It primarily involves absorption of UV light by electrons in a molecule's frontier orbital [4]. Thus, the active compound in sunscreens protects the skin from sunburn by blocking UV radiation. The extent of this action can be evaluated experimentally based on the UV-Vis absorption spectrum. Therefore, a knowledge of the nature of UV filter action, the straightforward identification of a target function (UV-Vis spectral area), together with the relative ease with which molecules of intermediate size can be modeled, makes the group of molecules that act as UV filters an ideal object for a QSAR-type study.

With the aim of introducing the QSAR methodology at undergraduate level, this paper describes a simplified *in silico* QSAR study for different UV filters. The model is developed using calculated numerical molecular descriptors that encode information about each molecular structure. From the different modeling strategies, the simple Multiple Linear Regression (MLR) has been selected to correlate the molecular descriptors and the sunlight blocking effect, in this case the full area under the UV-Vis spectrum. In order to allow completion of the project within a reasonable time, some simplifications have been made to obtain the molecular descriptors. Thus, the theoretical method employed to generate both the molecular descriptors and the UV-Vis spectral area are based on semi-empirical quantum chemical methods. Moreover, the solvent effect is not taken into account [5]. Modeling of the solvatochromic effect is a complex undertaking and is outside the didactical scope of the present paper [6]. Therefore, the conclusions that can be drawn are somewhat limited. Notwithstanding, the basic steps in QSAR methodology, *viz.*, the building up and optimization of 3D molecular structures, generation and selection of descriptors and model construction and validation are demonstrated and analyzed.

This paper therefore explores the quantitative relationship between absorption in the UV-Vis region with the chemical structure of UV filters, without taking into account possible spectral shifts due to the presence of a solvent.

2. Methodology

The sun protection mechanism using organic chemicals is based on the strong absorption of UV light by these molecules. Therefore, the molecular energy gap for the frontier orbital set close to HOMO-LUMO should have a value in the UV-Vis range. This energy gap can be realized with aromatic compounds having conjugated C=C double

bonds and other diverse functional groups. The UV-Vis absorption interval and strength can be modified by varying the type and position of molecular substituents. The entire project can be developed in several stages.

2.1. Data Set Selection

The selection of compounds that constitute the data set should be the first step of the project. Mainly seven different classes of organic compounds are commonly employed as active UV filters, Figure 1, shows their basic schematic structures. The compound data set for this study was selected from the globally approved list of UV-Vis filters [7, 8].

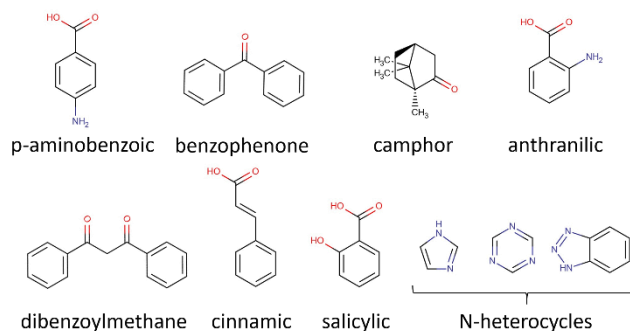


Figure 1. Schematics structures of different classes of organic compounds, containing conjugated double bonds, frequently used as UV filters

The set contains five *p* aminobenzoate derivatives (PABAs), twelve benzophenone derivatives, six camphor derivatives, three dibenzoylmethane derivatives, eleven cinnamate derivatives, six salicylate derivatives, ten N-heterocyclic derivatives (imidazole, triazine, benzotriazole, ...), one anthranilate and two miscellaneous compounds (beta-carotene and melanin). The table of data can be obtained from the authors upon request.

2.2. Molecular Computer File Generation

For each compound, a computer file containing the molecular structure readable by computational molecular programs should be generated. Common molecular files read by the majority of the computational chemistry programs are the mol file, MDL and structure data file, SDF [9]. Computational Chemistry for Chemistry Educators [10], offers information and resources for molecular modeling, with systematic instructions for molecular modeling with different softwares. From the name of each organic compound, a computer file was generated containing the 3D initial molecular structure. Different web resources can be employed to obtain the text file containing the molecular structure, from the IUPAC name and/or using the "simplified molecular-input line-entry system", SMILES [11]. To avoid issues arising from different nomenclature and/or isotopes, each compound is identified by its unique CAS registration number [12]. This registry can be obtained from CACTUS (CADD Group Chemoinformatics Tools and User Services) [13]. From CAS a standard molecular file can be exported using the ChemSpider [14], ChemCell [15], now also available on Google Spreadsheets, or Chemicalize [16] web

resources. Among them, ChemSpider, Chemicalize and PubChem are recommended, they offer web links that give access to estimates of assorted molecular properties, or descriptors in QSAR nomenclature, from its structure: ACD/Labs [17], EPISuite [18], ChemAxon [19] and Mcule [20].

2.3. Theoretical UV-Vis Spectra and Selection of Computational Method

The sunblock protection efficiency is usually characterized by a test *in vivo*. Estimation of the sun protection factor, SPF, is based on the ratio of the minimum erythematic dose between protected and unprotected skin. The comparable parameter used *in vitro* does not have a unique and widely accepted definition. In this paper, the modified parameter defined by UV area per unit of wavelength [21], recommended based on FDA regulations [7], is used:

$$\text{UV area per unit of } \lambda \text{ (L/(mol cm))} = \frac{\int_{\lambda_1}^{\lambda_2} \varepsilon(\lambda) d\lambda}{\lambda_2 - \lambda_1} \quad (1)$$

where $\varepsilon(\lambda)$ is the extinction coefficient and λ is the wavelength. This target parameter can be easily estimated from experimental or theoretically generated UV-Vis spectra.

The theoretical UV-spectrum can be generated by computational methods using the approximation known as configuration interaction, CI, [22]. The transition energy between the ground and the excited states are computed for the same geometry, that of the ground state. This energy is given usually as a wavelength for each allowed electronic transition. The relative intensity for each transition is related to the change in the dipolar moment strength and is reported as the oscillator strength for each electronic transition [23]. Forbidden transitions have an oscillator strength value close to zero. For each active transition (i), the extinction coefficient is produced as a Gaussian band shape, with a constant half-width (approx. 0.4 eV) by using the method proposed in Gaussian Tech Notes [24]:

$$\varepsilon_i(\lambda) = 1.3062974 \times 10^8 \frac{f_{\max,i}}{\sigma(\text{cm}^{-1})} \exp \left[- \left(\frac{1/\lambda - 1/\lambda_{\max,i}(\text{nm})}{\sigma} \right)^2 \right]$$

$$\sigma = 0.4 \text{ eV} = 1/3099.6 \text{ nm}^{-1} = 10^7 / 3099.6 \text{ cm}^{-1} = 3.22622 \times 10^3 \text{ cm}^{-1} \quad (2)$$

where $f_{\max,i}$ and $\lambda_{\max,i}$ are the oscillator strength and the wavelength (nm) of the electronic state i , respectively.

The full spectrum can be easily convoluted by adding all active transitions in the UV-Vis energy interval:

$$\varepsilon(\lambda) = \sum_i \varepsilon_i(\lambda_i) \quad (3)$$

Finally, the UV area is obtained from the spreadsheet-generated spectra by integration using the trapezoid rule.

The ground state molecular geometry can be optimized by

several computational methods: molecular mechanical, semi-empirical [25] and by Density Functional Theory (DFT) [26].

Additionally, the solvatochromic effect is an experimental complication *in vitro* when we want to compare the sunblock effectiveness *in vivo* [5]. A deeper theoretical study should be performed in order to obtain UV-Vis spectra closer to those obtained experimentally. Nevertheless, this consideration is outside the scope of the present paper, which is meant to be an introduction to the QSAR methodology at the undergraduate level.

2.4. Estimating Molecular Properties

The ability to predict properties depends strongly on an appropriate choice of descriptors. There is a variety of molecular properties that can be used in QSAR. They can be classified as physicochemical [27, 28] and topological [29], so that in turn they can be divided into groups [30-32]:

- Constitutional (number and type of atoms, rings, MW, ...)
- Topological (indices that represent the structure using graphs)
- Geometric (Areas, volumes, ...)
- Mechanical (moments of inertia, ...)
- Electrostatic (polarizability, partial charge, dipole moment, ...)
- Quantum (frontier molecular orbitals, free valence, bond order, electronic energy, electrostatic interaction, ...)
- Thermodynamic (heat of formation, heat capacity, ...)

Nevertheless, there is a wide variety of software applications to obtain molecular descriptors: Codessa Pro [33], Dragon 6 [34], CORINA Symphony [35], and Molecular Operating Environment [36]. Most of them provide more than 1000 descriptors for any molecule. However, the use of a large number of descriptors in the construction of the model has, in addition to increasing computing time, two disadvantages: increase of 'noise', due to the use of some correlated descriptors, and model 'over-training'. The latter tend to produce models with low predictive power. Nevertheless, most of the above-mentioned software provides tools for fast data screening to obtain the most significant descriptors, minimizing the above-mentioned adverse effects.

2.5. QSAR Model Construction

The first stage in the model building process will be the selection of variables (properties) that could contribute significantly to the model as well as the estimation of their level of importance.

These properties can be grouped in matrix form, where each column is associated with a specific property and each row corresponds to a chemical compound. These properties are considered as independent variables, termed an X matrix. An additional column is incorporated containing the dependent variable: a molecular property (experimentally

determined or theoretically calculated) to be replicated by the model, the Y matrix. The analysis of this matrix equation is performed depending on the types of variables and their mathematical relationship. Thus, the following types of fundamental modeling strategies have been considered in the chemometric literature [37, 38]:

- MLR, Multiple Linear Regression
- PCR, Principal Component Regression
- PLS, Partial Least Squares
- TFA, Target Factor Analysis
- ANN, Artificial Neural Networks
- SVM, Support Vector Machines

If it can be assumed that the selected independent properties mainly contribute linearly to the model, the multiple linear regression (MLR) based on the least squares method should be the model technique of choice. This model can only be applied when the variables have low synergy among them, and no quadratic terms need to be considered.

With a view to the pedagogical scope of the project, students mainly employed MLR which can also be easily handled by Excel. Therefore, the MLR model equation, in matrix format, will be:

$$Y = X \cdot B + E \quad (4)$$

where Y is the dependent variable matrix, in this case, the UV area per unit of wavelength; X is the independent variable matrix, containing molecular properties; B corresponds to the regression coefficient matrix, and E is associated to the residual error matrix.

The regression coefficient matrix, B , the response matrix Y and residual error matrix can be estimated by least squares analysis:

$$Y = X \cdot B \Rightarrow X^T \cdot Y = X^T \cdot X \cdot B \Rightarrow B = (X^T \cdot X)^{-1} \cdot X^T \cdot Y \quad (5)$$

$$Y = X \cdot B = X \cdot (X^T \cdot X)^{-1} \cdot X^T \cdot Y = H \cdot Y \Rightarrow E = Y - Y$$

where the superscript T stands for the transposed matrix and the superscript -1 for the inverse matrix operation, respectively. The tests for degrees of significance for the linear model and for the coefficients are performed by the statistics Snedecor's F and Student's t, respectively [39].

Additionally, application of the MLR model has some statistical prerequisites: the residuals should be normally distributed, with a constant variance and not show any trends when plotted against any independent variable. These prerequisites can be checked by any statistical software, like SPSS [40] or Statistica [41]. These statistical tools can also assist in the model building by including or dropping variables by stepping forward or backward in the model, respectively.

Furthermore, a severe problem in using the MLR procedure occurs if there is a degree of measurable correlation between some of the supposedly independent selected variables. In particular, difficulties arise in the calculation of the inverse of the correlation matrix:

$$C = X^T X \quad (6)$$

Each element in the correlation matrix indicates the degree of correlation between the two variables. All diagonal elements are equal to unity, expressing the complete correlation for each variable with itself. Entries of the correlation matrix that are close to zero is an indication that the corresponding two variables are uncorrelated. Several strategies can be employed to minimize the correlation issues. The correlation matrix analysis is the simplest way, selecting one variable from each group that is highly correlated (absolute values higher than 0.6) and dropping the rest of the group. Nevertheless, this strategy can lead to the loss of some information contained in the correlated variables. Therefore, more complex strategies of modelling should be performed such as principal component regression or partial least squares.

3. Results and Discussion

After compound selection, the molecular file with the molecular structure was generated from the web facilities described above.

In the present project the CAChe 7.5 software as "all-in-one" [42] has been employed. CAChe, computer-aided chemistry, is a 3D molecular modeling tool environment capable to build up molecules. The program performs molecular calculations, named "experiments", using classical and quantum mechanical theories providing electronic properties of the optimized molecular geometry. Moreover, the software provides a separate "ProjectLeader", as spreadsheet interface to perform batch-processing calculations for several chemical samples at the same time (structures, properties, statistical analyses, multiple linear regression, calculations based on customizable equations ...). This separate tool is specially adequate and comfortable to perform QSAR studies. Using this spreadsheet interface the table with the molecular properties for each molecule can be built up.

Table 1. Selected molecular properties for the Sunscreens. Procedures and literature from [42]

Molecular Weight
Count: Atoms (Nitrogen, Oxygen); Bonds (Double bonds); Ring (All rings, Aromatic)
Dipole Moment (Debye)
Polarizability (Å ³)
HOMO Energy (eV)
LUMO Energy (eV)
Energy gap LUMO-HOMO (eV)
Lambda Max UV-Visible (nm)
Connectivity Index (order 0, 1, and 2)
Valence Connectivity Index (order 0, 1 and 2)
Log P (Partition Octanol/Water)
Heat of Formation (kcal/mole)
Total Energy (Hartree)

The generation of the UV-Vis spectrum was performed by the technique of configuration interaction, CI, described above, selecting “the experiment” UV-visible transitions. This experiment can be performed using different computational methods, in our case ZINDO and PM5.

A simplified flow diagram showing the step by step procedure and tools employed to generate the data matrix X , target matrix Y and the model building, is showed in Appendix I. A complete file in Excel format can be obtained from the authors upon request.

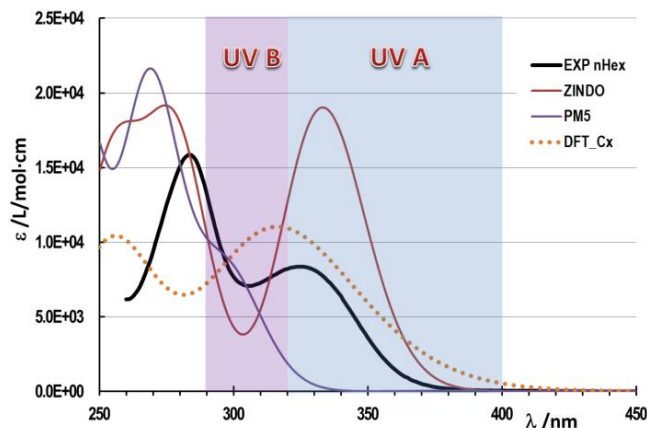


Figure 2. Oxybenzone experimental UV-Vis spectrum in n-Hexane compared with that theoretically calculated using different computational methods ZINDO and PM5 in vacuum and DFT in cyclohexane, modelled as a continuum with uniform dielectric constant

From the sunscreen chemicals essayed, Oxybenzone shows a very low experimental solvatochromic shift [21]. Thus, it has been selected as a suitable prototype compound to compare different theoretical computational methods. The solvent effect has been simulated in the literature by using the self-consistent reaction field (SCRF), where the solvent is considered a dielectric continuum with constant permittivity and refractive index [43]. Figure 2 shows the Oxybenzone experimental UV-Vis spectrum obtained in n-Hexane compared with some theoretically estimated spectra by using different computational methods. The experimental spectrum is different from all those obtained with the computational methods tested. Moreover, the

sunscreen's solvatochromic shift, between experimental and computed, agree only in sign but not in magnitude.

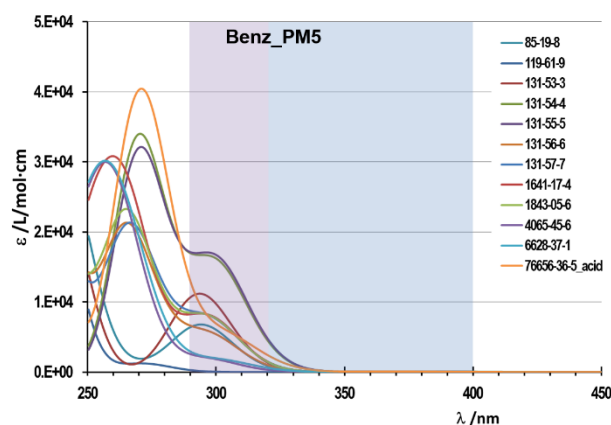
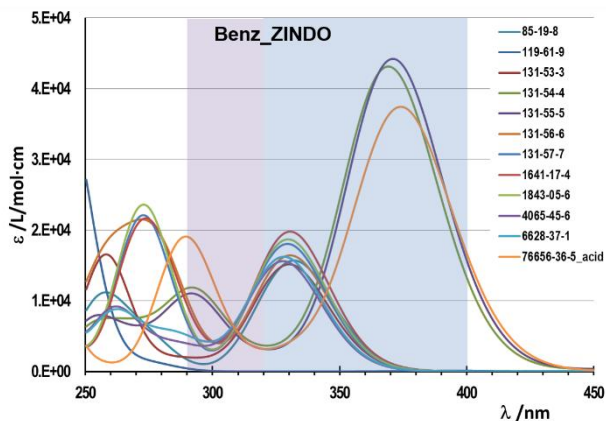
INDO and PM5 were the semi-empirical computational methods selected for both the ground state molecular geometry and properties estimation. ZINDO [44] developed from INDO/S semi-empirical method has a specific parameterization for electronic (UV-Visible) spectra, producing good results at low computational cost and has been selected for the UV-Vis spectra generation. DFT methods have a high ‘computational cost’ when compared with semi-empirical calculations (500 to 1000 times). This aspect, use of DFT methodology, and the solvent influence could be applied to developing post-graduate projects (at Masters level).

As was stated before, the solvent model inclusion is a complex task and the solvent effect is different for the different molecules, the various solvents, and their properties. Solute-solvent interactions are a complex matter even from the empirical point of view [45]. Performing the calculations “in vacuum”, simplifies and speeds up the calculation and, in a way, focalizes on how the intrinsic molecule structure influences the UV-Vis area. Thus, all the molecular calculations for the analysis have been carried out in vacuum.

Most of the theoretical UV-Vis spectra (250 nm- 400 nm, 0.5nm step) obtained are shifted to higher energies when compared with the experimental spectra obtained in non-polar solvents such as n-hexane or cyclohexane [21].

From the theoretical generated UV-Vis spectra, a spreadsheet has been used to estimate the UV area for each compound by the well-known trapezoid rule after selecting the appropriate wavelength interval (290-400 nm).

The PM5 method shifts the absorption peaks to higher energies, pushing the compound spectra to the UVC zone and therefore, lowering the area and the magnitude of the target function, the area under UVA and UVB, see Figure 3. The model analysis could be done by selecting a broader wavelength interval (250 nm to 400 nm) so as to obtain substantial differences among compounds of the same group. After trying this approach, i.e. widening the wavelength interval, no significant improvements were achieved.



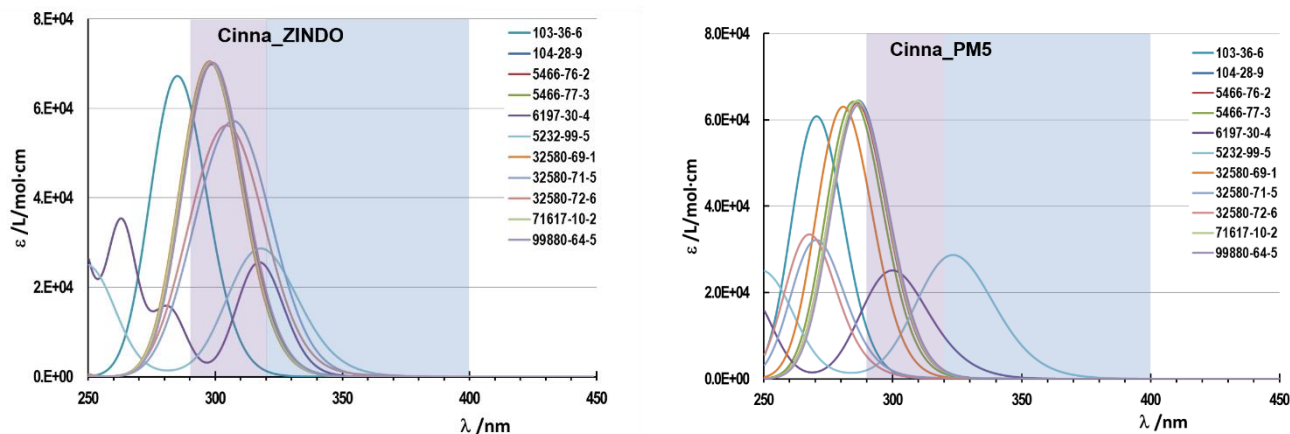


Figure 3. UV-Vis spectra of Benzophenones (Benz) and Cinnamates (Cinna) obtained with different semi-empirical computational methods: left ZINDO, right PM5. Each compound is identified by the CAS #

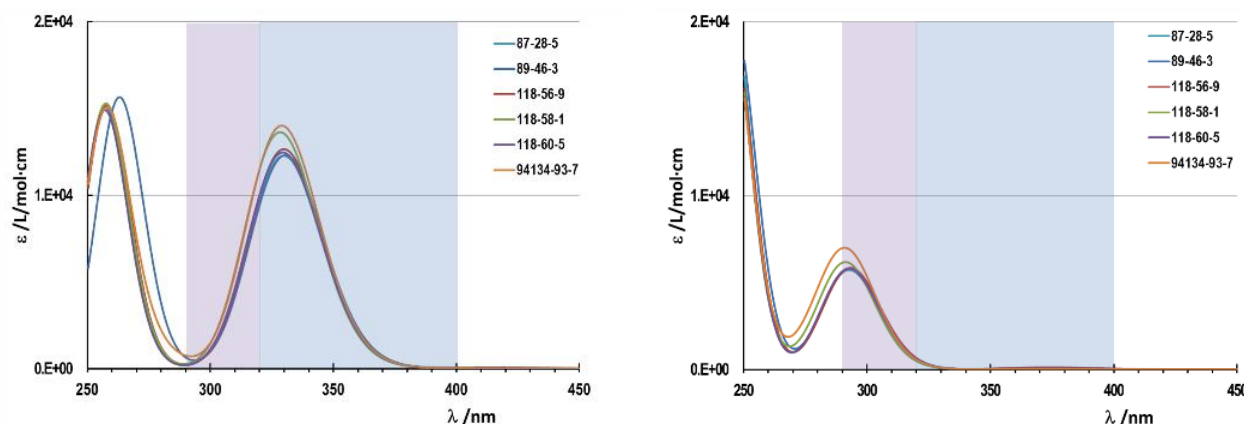


Figure 4. UV-Vis spectra for salicylates obtained by ZINDO with different geometry. Left, spectra with intramolecular H-bond between the oxygen of the carbonyl group and the hydrogen of the phenol group. Right, spectra without intramolecular H-bond

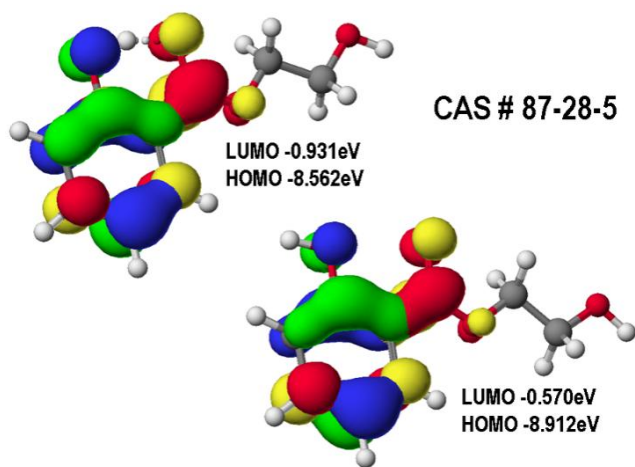


Figure 5. Frontier orbitals shown as electron isodensity surfaces (HOMO (blue-green), LUMO (red-yellow)) for 2-hydroxyethyl salicylate with and without intramolecular H bond, $\text{C=O}\cdots\text{H-O}$

No conformational study was done to obtain the conformer configuration with lower energy. The initial molecular geometry optimization was generated from molecular mechanics considerations. However, the structure of some compounds could have a tendency to form intramolecular H-bonds, especially in nonpolar solvents.

Two different molecular structures for salicylates were optimized by ZINDO. Figure 4 shows the differences in the UV-Vis spectra optimized with and without H-bond between the hydrogen of the phenol group and the oxygen of carbonyl group. The spectra generated from the structure with the intramolecular H-bond shows behavior that more closely agrees with that found experimentally [46]. Consequently, the molecular geometries of these compounds have been optimized in a conformation capable to form an intramolecular H-bond.

Figure 5 shows the small differences in the frontier orbitals for the two structures of 2-hydroxyethyl salicylate (CAS# 87-28-5). The energy gap between HOMO and LUMO is smaller for the molecule with intramolecular H-bond, 7.631eV, compared with 8.342eV for the other conformer without H-bond.

Moreover, the molecular geometry optimization of the benzophenones group was re-checked. In some cases, the optimal molecular structure is non-planar. The dihedral angle between the aromatics rings can be larger than 40 degrees to avoid the steric effect from the aromatics rings. Nevertheless, it is possible to attain an optimal planar configuration if the angle formed between the carbon atom of the carbonyl group and the two adjacent carbons, usually

120 degrees with classical molecular mechanics, is a bit larger than 120 degrees. In this case, a near-planar benzophenone molecular structure can be optimized. This planar structure gives lower energy values for the LUMO virtual orbital, shifting the HOMO/LUMO gap to larger wavelengths.

Thus, two different groups of molecular geometries have been employed in the modeling, salicylates with and without intramolecular hydrogen bonds and benzophenones with and without planar geometry.

3.1. MLR Model Building

Before starting the modeling, close data scrutiny will have to be the first step. Simple statistical analysis (number of valid data, mean, standard deviation...) can help to detect possible codification errors and outliers. The use of the “box and whisker” plots is recommended for discovering spurious and suspicious values, ultimately simplifying and improving the analysis.

Thus, in the actual statistical analysis of a data set, when considering the property molecular weight (MW), compounds with values exceeding 500 Daltons should be considered as suspicious outliers. Additionally, those molecular properties that have a close relationship with the MW will also have suspicious values for this group of compounds. However, this group should not be removed from the data set because they represent the new generation of sunscreen compounds. Compounds obeying the 500 Da rule have lower skin absorption and toxicity level [47], and so, they are preferred in the sunscreen formulation.

Another important preliminary and necessary analysis is

the inspection of the correlation matrix, Eqn. 6. This matrix can be easily obtained from the spreadsheet matrix multiply function between the transposed matrix of molecular properties and the original molecular properties matrix.

Table 2, gathers the correlation values for some molecular properties. To facilitate their analysis, cells with a correlation level greater than 0.6 have been given different colors. Thus, some molecular properties show a moderate degree of correlation with several other: MW, Log P, #Nitrogen, #Oxygen, Connectivity Index 1, Heat of formation...

The usual recommendation, to minimize errors in the modeling, should be the selection of just one property of the group of properties that is highly correlated. The use of principal component analysis, PCA, can help to classify the different properties observing their values in the principal component space [48]. Moreover, PCA can also detect hidden phenomena by reducing the number of properties to be used in finding the most important ones. The reduction of variables and their analysis were not performed by the students in the development of the project.

Figure 6 shows some molecular properties projected in the plane corresponding to the two first principal components. It is observed that the properties related to frontier orbitals and the dipole moment are not grouped in the same quadrant. The rest of molecular properties seem to have similar coordinates (loadings), indicating their comparable contribution to the factors. In view of this plot analysis, the molecular properties that are not directly related with the electronic distribution seem to provide nearly the same information, and they should be treated as a single property.

Table 2. Correlation matrix for some selected molecular properties. Colored cells indicate a correlation higher than 0.6

	ΔH_f	HOMO	Dipo.	Lamb.	GAP	#N	#Rng	LogP	VC2	#ARng	#2Bnd	#O	VC1	Polar.	VC0	CI1	MW
ΔH_f	1.0	-0.3	0.2	0.3	0.2	0.8	0.2	0.6	0.5	-0.5	-0.5	0.9	-0.7	0.5	-0.2	0.6	0.7
HOMO	-0.3	1.0	-0.4	-0.4	0.3	-0.3	-0.4	-0.4	0.0	0.0	0.4	-0.3	-0.1	0.0	0.0	-0.4	-0.1
Dipole	0.2	-0.4	1.0	-0.1	-0.5	0.1	-0.1	0.3	0.2	-0.3	-0.1	0.1	-0.1	0.1	-0.3	0.3	0.2
Lambda	0.3	-0.4	-0.1	1.0	0.4	0.3	0.5	0.5	0.0	0.2	-0.4	0.5	0.0	0.0	0.2	0.4	0.0
GAP	0.2	0.3	-0.5	0.4	1.0	0.2	0.2	0.1	-0.1	0.3	-0.1	0.3	-0.1	0.3	0.3	-0.2	0.1
#N	0.8	-0.3	0.1	0.3	0.2	1.0	0.5	0.8	0.4	-0.6	-0.1	0.9	-0.3	0.4	0.1	0.6	0.3
#Ring	0.2	-0.4	-0.1	0.5	0.2	0.5	1.0	0.5	-0.4	0.0	-0.1	0.5	0.4	0.0	0.5	0.2	-0.3
Log P	0.6	-0.4	0.3	0.5	0.1	0.8	0.5	1.0	0.3	-0.5	-0.2	0.8	-0.2	0.1	0.0	0.6	0.2
VC2	0.5	0.0	0.2	0.0	-0.1	0.4	-0.4	0.3	1.0	-0.6	0.0	0.3	-0.9	0.3	-0.4	0.6	0.4
#ARing	-0.5	0.0	-0.3	0.2	0.3	-0.6	0.0	-0.5	-0.6	1.0	-0.3	-0.5	0.4	-0.3	0.2	-0.5	-0.3
#2Bond	-0.5	0.4	-0.1	-0.4	-0.1	-0.1	-0.1	-0.2	0.0	-0.3	1.0	-0.2	0.3	-0.1	0.4	-0.2	-0.7
#O	0.9	-0.3	0.1	0.5	0.3	0.9	0.5	0.8	0.3	-0.5	-0.2	1.0	-0.4	0.5	0.1	0.6	0.3
VC1	-0.7	-0.1	-0.1	0.0	-0.1	-0.3	0.4	-0.2	-0.9	0.4	0.3	-0.4	1.0	-0.4	0.4	-0.4	-0.7
Polariz	0.5	0.0	0.1	0.0	0.3	0.4	0.0	0.1	0.3	-0.3	-0.1	0.5	-0.4	1.0	-0.3	-0.1	0.4
VC0	-0.2	0.0	-0.3	0.2	0.3	0.1	0.5	0.0	-0.4	0.2	0.4	0.1	0.4	-0.3	1.0	0.0	-0.7
CI1	0.6	-0.4	0.3	0.4	-0.2	0.6	0.2	0.6	0.6	-0.5	-0.2	0.6	-0.4	-0.1	0.0	1.0	0.2
MW	0.7	-0.1	0.2	0.0	0.1	0.3	-0.3	0.2	0.4	-0.3	-0.7	0.3	-0.7	0.4	-0.7	0.2	1.0

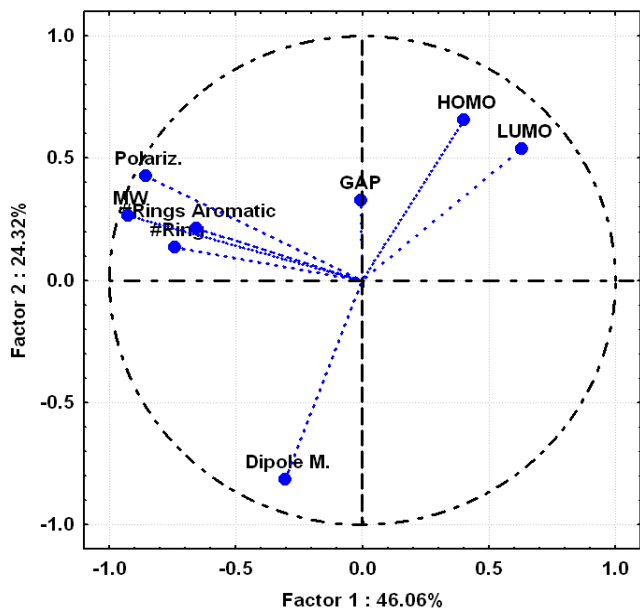


Figure 6. Projections of the molecular properties (variables) on the two first principal components plane

Therefore, before modeling by multilinear regression (MLR) three basic requirements should be met. The data analysis to locate possible outliers, since MLR is susceptible to them. The correlation analysis to minimize the “noisy” data. Parameters as tolerance, $T=1-R^2$, or its inverse, the Variance Inflation Factor, $VIF = 1/T$, are commonly used in statistical software to easily identify the correlation. Tolerance values under 0.2 ($VIF=5$), indicates a high degree of multicollinearity. In the correlation matrix depicted in Table 2, T values below 0.4 have been colored to indicate some degree of correlation between the properties. Moreover, MLR assumes a linear relationship between the independent and dependent variables. The linearity assumption can best be tested with scatterplots with properties. Mathematical transformation of the variables that show no linear behavior is the common method employed. Logarithm, inverse, square are typical variable transformations to correct for non-linearity.

Moreover, two additional prerequisites should be checked to satisfy to application of the least squares method used in MLR. Most of these conditions can be performed by means of residuals analysis:

- The variables (properties) should have a normal distribution. This can be verified by checking that the histogram of residuals has approximately a normal distribution.
- Constant variance of error terms for the independent variables, known as homoscedasticity. The diagnostic is based on the detection of a pattern on the residuals vs. the property to be evaluated (dependent variable).

To satisfy these last two requirements, the standard procedure is again mathematical transformation of variables. Finally, yet importantly, the MLR analysis requires a sample size of over five cases per independent variable.

Some statistical procedures can be used to select the number of independent properties to be included in the best MLR model [40, 41]. The backward stepwise procedure starts by including all properties in the model. In each next step, the smallest significant property is removed until a reduction in the model performance is detected. The usual halting criterion is a combination of statistical F-Snedecor and Student's t tests. The forward step starts by including in the model the more significant property. In the successive steps, a new property is added and a similar statistical criterion is employed to stop the addition of properties. In addition, a combined method can be applied where in each step the properties are tested to be included or excluded. All these “wise” procedures may be subject to some degree of criticism because they are prone to producing over fitted models with low predictive power. The data are split into two different groups. One, the training set (70% of data), is used to build up the model and the rest of the data (30%), unknowns for the model building, constitute the test group by means of which the predictive power can be evaluated. These statistical procedures were not employed in this project by the students, but there is no doubt that their use and analysis constitute another important topic of study in QSAR model building for graduate students. In this project, the forward step for the full data and only the best single regression for each group of compounds have been used, mainly due to the relatively low number of sunscreens commonly in use.

Figure 7, shows a scatter plot of the UV area by wavelength (SPF *in vitro*) theoretically generated versus the ones estimated from the molecular properties by MRL forward stepwise for the 53 sunscreens that were analyzed. The analysis showed a close correspondence for the data set containing the planar molecular geometry for benzophenones and with an intramolecular hydrogen bond for the salicylates.

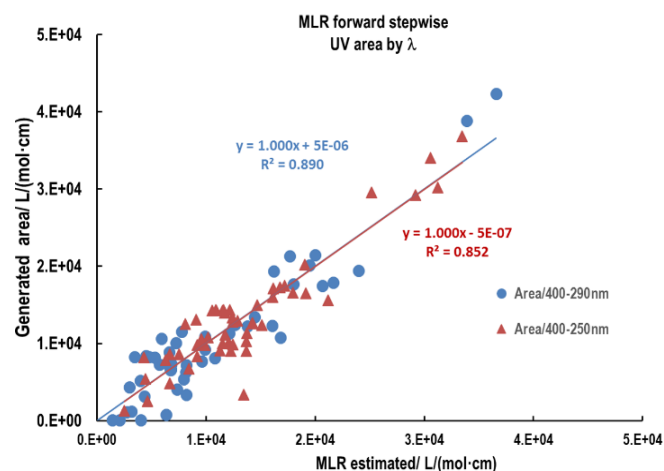


Figure 7. Sunscreen scatter plot of UV area by wavelength of theoretically generated (ZINDO) versus the corresponding areas estimated by MLR forward stepwise. Blue dots correspond for the area calculated for the spectral range from 290nm to 400nm and red triangles the area calculated for the 250nm to 400nm interval

As was stated before, theoretical semi-empirical methods employed (PM5 and INDO) tend to shift the absorption peaks to shorter wavelength, into the UVC zone, if the spectra are compared with those obtained experimentally in nonpolar solvents. Thus, a lower sensitivity of the area under the UVA and UVB zones is obtained. This is especially true for the PM5 method, where the UV peaks are localized below 280nm. Nevertheless, in order to compensate for this theoretical spectral shift, the spectral area was also estimated for a broader wavelength interval (250nm to 400nm) using the ZINDO method. This area estimation provides larger areas and therefore an increase in the sensitivity in the variability among the compounds when part of the UVC spectra is included in the generated area.

The relevant molecular properties that contribute significantly to the MLR model, for the reduced wavelength interval (290-400nm) are the total number of rings (#Rng), the number of aromatic rings (#ARng), the dipole moment (Dipole) and the HOMO/LUMO energy gap (GAP):

$$\begin{aligned} \text{Area}/\lambda_{(290-400\text{nm})} &= 1.02 \cdot 10^3 * (\#Rng) + 2.17 \cdot 10^3 * (\#ARng) \\ &+ 6.76 \cdot 10^2 * (\text{Dipole}) - 1.38 \cdot 10^4 * (\text{GAP}) + 1.03 \cdot 10^5 \quad (7) \\ \text{RCV}^2 &= 0.839 \quad R^2 = 0.890 \end{aligned}$$

Figure 7 reveals a lack of significant differences, in terms of correlation coefficient, when the wider UV interval is employed. Nevertheless, except for variable HOMO/LUMO energy gaps, the type of variables involved in the model changes. Now, the number of nitrogen atoms, the valence connectivity index 2, the heat of formation and the GAP are significant:

$$\begin{aligned} \text{Area} / \lambda_{(250-400\text{nm})} &= 1.42 \cdot 10^3 * (\#N) - 6.88 \cdot 10^3 * (\text{GAP}) \\ &- 3.62 \cdot 10^2 * (\text{VC}2) - 58 * (\Delta H_f) + 5.64 \cdot 10^4 \quad (8) \\ \text{RCV}^2 &= 0.833 \quad R^2 = 0.853 \end{aligned}$$

Thus, for the sake of simplicity, only the reduced wavelength interval, (290nm-400nm) data set will be analyzed.

When the whole data set is built up using the benzophenones molecular group without necessarily considering their planar molecular structure, slightly lower regression coefficients (R^2) are obtained (approx. 0.85), but basically the same set of properties describe the MLR model: number of all rings (#Rng), number of aromatic rings (#ARng) and HOMO/LUMO energy gap (GAP).

When the entire data set is built up without considering the possibility of intramolecular hydrogen bonding for the group of salicylates, the regression coefficients decrease significantly down to 0.6 if the same number of molecular properties is included in the MLR model.

Table 3 collects a summary of the best single linear regression analysis for the different groups of compounds. There is no sense to apply the MLR model methodology to each group of compounds considering the low number of items in each group.

The correlation coefficient and RCV^2 for salicylates group without considering the intramolecular H bond is a projection of the observed right spectra in Figure 4. The spectral areas for the 290nm to 400nm interval are small and very similar for the entire molecular group. Nevertheless, this group of molecules with the intramolecular H bond produces larger area values in the UVA spectral zone and with some differences among the salicylates molecules. These facts are reflected in better linear regression parameters R^2 and RCV^2 obtained when considering the intramolecular H bond.

Table 3. Best simple linear regression parameters for each molecular group

Compound group	# items	Property	R^2	RCV^2
PABAs	5	GAP	0.832	0.632
Benzophenones (Planar)	12	GAP	0.941	0.853
Benzophenones	12	GAP	0.931	0.784
Camphors	6	GAP	0.912	0.802
Cinnamates	11	HOMO	0.843	0.800
Salicylates (H Bond)	6	#Double bonds	0.908	0.747
Salicylates	6	Valence Conn.2	0.486	No variance
N-Heterocycles (Mix)	10	#ARing	0.566	0.510

On the other hand, the molecular property listed in Table 3 as having high significant linear correlation coefficients seems to be different for the various molecular groups. Thus, for p aminobenzoic acid, benzophenone and camphor derivatives the HOMO/LUMO energy gap (GAP) is the optimal molecular property that describes the linear relationship. The best linear molecular property is not the same one for rest of the molecular groups. A possible explanation could be found if an extensive analysis of UV spectra theoretically computed for each molecular group is done. The position of the maximum wavelength and its corresponding area for the HOMO/LUMO transition are decisive in determining the contribution to the GAP parameter. Thus, for benzophenones derivatives the HOMO/LUMO transitions have maxima at wavelengths over 340nm with a large extinction coefficient, so the GAP parameter mainly contributes to the UV area. The salicylates group also has maxima at wavelengths over 330nm, but their extinction coefficients are approximately four times lower as compared with the benzophenones group. Therefore, the contribution to the UV area of the GAP parameter is lower. Cinnamates derivatives have large extinction coefficients, but the wavelengths at maxima are close to the UVB limit (290nm). Finally, the N-heterocycles is a group of compounds of a very different nature, (imidazole, benzodiazole, triazin, ...) with very diverse parameter values for maximum wavelengths and extinction coefficients and could be expected to have low linear correlation coefficients.

One step forward in the results analysis, not carried out by the students in the project, is the Principal Component Regression. This method combines the Principal Component Analysis with MLR avoiding the multicollinearity issues. PCR has been performed gradually using SPSS [40], following the example reported by Liu *et al.* [49] Moreover, none of the possible concerns expressed by Hadi and Ling in [50] about their use are applicable in this study. In the first step, the variables are statistically analyzed to fulfill the MRL requirements and the correlated variables are dropped. The factor analysis step indicates that seven principal components are necessary to obtain nearly 100% of the explained variance. This could be an indication that some extra variables are needed in the model. The best model PCR obtained provides a $R^2=0.883$. The significant variables in this model in order of their importance are, HOMO/LUMO gap, wavelength with higher extinction coefficient, dipole moment, number of molecular rings, number of double bonds and number of oxygen atoms. Thus, a very similar model is obtained with this more sophisticated procedure.

Finally, taken into account the undergraduate framework in question, some remarks are in order regarding the present study. The number of molecules has been limited to the chemicals that have been internationally approved for use as sun blockers. The undergraduate character of the project, as well as time constraints, limited the level of quantum calculations and the inclusion of solvent effects. Moreover, a deeper analysis of the obtained area under the UV-Vis (dependent variable) indicates that in some compounds there are important contributions to this area by UV-Vis transitions different from those associated with the HOMO-LUMO gap. Thus, these facts will likely have a negative impact on simple linear model building. Notwithstanding these limitations, the various tools and procedures used by the students in building the QSAR model have provided a useful experience by showing them how different tools and areas of chemistry can be combined to obtain a near quantitative prediction of activities of compounds from their chemical structure.

4. Conclusions

Modeling *in silico* UV-Vis spectra can be performed by the configuration interaction singles (CI-s), a relatively low-level computational method for computing excited states. The project ambit, graduate level, simple organic molecules, together with the possible computational limitations, motivated the selection of a semi-empirical theoretical method for molecular modeling.

Moreover, the UV-Vis spectrum is not influenced only by the compound itself but also by its environment, such as the solvent, solution pH, etc. These facts introduce some degree of difficulty that have prevented QSAR studies from being more widely used in chemical education.

Nevertheless, among the various semi-empirical methods, ZINDO has parameters designed to match the UV-Vis

spectra. Despite the shift of the maxima in the case of some spectra, the correct overall trend for the full UV-Vis spectra of simple organic molecules can be obtained.

Additionally, the 2D-QSAR study is mainly concerned with the correlation between the simple molecular structure descriptors and the UV-Vis spectral area. Thus, in spite of using approximate molecular modeling, the application of this methodology has a reasonable basis. QSAR analysis compares relative contributions and it is expected that the method employed provides approximately the same shifts for all molecules studied.

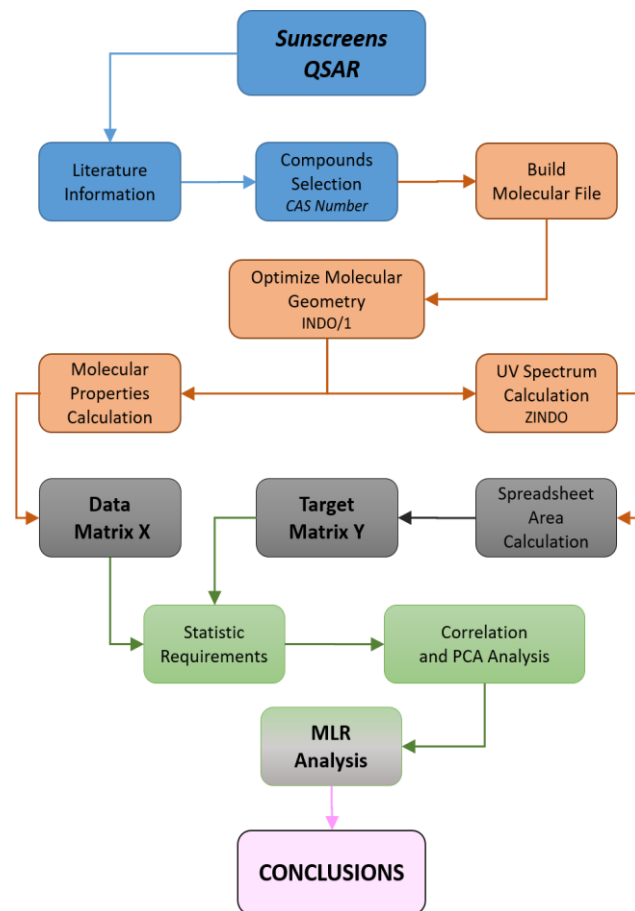
Therefore, this *in silico* QSAR study of sunscreens can be a good starting point to introduce the QSAR methodology at the final year undergraduate level. Nevertheless, limitations of its applicability should be clearly pointed out.

ACKNOWLEDGEMENTS

The authors are very grateful to Prof. R. Rodríguez Pappalardo for his helpful comments and suggestions. We also thank to students of Chemistry: A. Martínez Pascual and A. Palacios Morillo for their dedication in developing part of the “Sunscreen Project”.

Appendix 1

In silico QSAR UV filters study



- QSAR topic selection (Blue section).
 - Update literature, SciFinder, Google scholar,...
 - Compounds collection, ref. 21 and literature cited therein, FDA regulations,...
 - Unequivocally identification by CAS Registry Number, ref 12.
 - Molecular modeling tool. CAChe, ref 42 (Orange section).
 - Molecular structure file generation.
 - From CAS registry #, the references 14 and 16 provide an initial molecular file to be read by CAChe.
 - Ground state molecular geometry is optimized by semi-empirical method INDO/1.
 - Estimation of molecular properties (Data matrix X), using CAChe ProjectLeader. Export to Excel format.
 - UV spectra generation.
 - Generate UV spectrum using Configuration Interaction, ref 22, and ZINDO, ref. 44.
 - Export a text file containing the UV-Vis spectrum at 1nm interval for each compound.
 - Spreadsheet calculations (Grey section).
 - Estimation of the UV area per unit of wavelength, eq. 1. The integral is estimated by using the trapezoidal rule (Target matrix Y).
 - Statistical calculations (Excel or statistical package, references 40 and 41) (Green section).
 - Initial matrix data scrutiny: codification errors, outliers values,...
 - Correlation matrix inspection, drop highly correlated molecular properties.
 - Principal Component Analysis, projection of molecular properties on factors space and estimation of maximum number of variables.
 - Modeling strategy selection: Multi Linear Regression (MLR).
 - Checking variable (molecular properties) for normal distribution and homoscedasticity.
 - Molecular properties selection in the model by using MRL forward stepwise.
 - Model cross-validation (not performed in this study).
 - Best simple linear regression for each class of organic UV filter.
 - Conclusions (Pink section)
 - Advantages and disadvantages of QSAR.
- MD; 2010. <https://www.fda.gov/ScienceResearch/SpecialTopics/CriticalPathInitiative/ucm204289.htm> (Accessed March, 2017).
- [3] European Chemicals Agency (ECHA), "QSAR Toolbox", <https://echa.europa.eu/support/oeqd-qsar-toolbox> (Accessed March, 2017).
- [4] Shaath, N.A., On the theory of ultraviolet absorption by sunscreen chemicals, 1987, *J. Soc. Cosmet. Chem.*, 82, 193-207.
- [5] Agrapidis-Paloympis, L. E., Nash R.A. and Shaath N.A., The effect of solvents on the ultraviolet absorbance of sunscreens, 1987, *J. Soc. Cosmet. Chem.*, 38, 209-221.
- [6] Reichardt, C., *Solvents and Solvent Effects: An introduction*, 2007, *Organic Process Research & Development*, 11, 105-113.
- [7] FDA, Sunscreen drug products for over-the-counter human use; final monograph, 2011. Federal Register 76/117, 35620-35665, USA. (Accessed March, 2017).
- [8] Stiefel C. and Schwack W., Photoprotection in changing times – UV filter efficacy and safety, sensitization processes and regulatory aspects, 2015, *Int. J. Cosmet. Sci.*, 37, 2-30.
- [9] Dalby, A., Nourse, J. G., Hounshell, W. D., Gushurst, A. K. I., Grier, D. L., Leland, B. A. and Laufer, J., Description of several chemical structure file formats used by computer programs developed at Molecular Design Limited, 1992, *Journal of Chemical Information and Modeling* 32 (3), 244-255.
- [10] National Computational Science Institute, "Software Comparison Chart", http://www.computationalscience.org/ccce/about/whats_new/SoftwareComparison%20Lab1.pdf and http://www.computationalscience.org/ccce/about/whats_new/summary.pdf (Accessed March, 2017).
- [11] Weininger D., SMILES, a chemical language and information system. 1. Intro-duction to methodology and encoding rules, 1988, *Journal of Chemical Information and Modeling* 28 (1), 31-6.
- [12] CAS Registry. <http://www.cas.org/content/chemical-substances> (Accessed March, 2017)
- [13] CACTUS. <https://cactus.nci.nih.gov/chemical/structure>. (Accessed March, 2017)
- [14] ChemSpider. <http://www.chemspider.com/Search.aspx>. (Accessed March, 2017)
- [15] ChemCell. <https://github.com/cdd/chemcell>. (Accessed March, 2017)
- [16] Chemicalize. <http://www.chemicalize.org/>. (Accessed March, 2017).
- [17] ACD/Labs. <http://www.acdlabs.com/products/percepta/predictors.php> (Accessed March, 2017).
- [18] EPI Suite. <https://www.epa.gov/tsca-screening-tools/epi-suite-etm-estimation-program-interface>. (Accessed March, 2017)
- [19] ChemAxon. <https://www.chemaxon.com/>. (Accessed March, 2017).
- [20] Mcule. <https://mcule.com/>. (Accessed March, 2017).

REFERENCES

- [1] Hansch, C., Maloney, P.P., Fujita, T. and Muir, R., Correlation of Biological Activity of Phenoxyacetic Acids with Hammett Substituent Constants and Partition Coefficients, 1962, *Nature*, 194, 178-180. doi:10.1038/194178b0.
- [2] Food and Drug Administration (FDA). Critical Path Initiative. US Department of Health and Human Services, Rockville,

- [21] González-Arjona, D., López-Pérez, G., Domínguez, M. M. and Cuesta van Looken, S., Study of Sunscreen Lotions, a Modular Chemistry Project, 2015, Journal of Laboratory Chemical Education, Vol. 3 No. 3, 44-52. doi:10.5923/j.lce.20150303.02.
- [22] J. B. Foresman and H. B. Schlegel, Application of the CI-Singles method in predicting the energy, properties and reactivity of molecules in their excited states. Recent experimental and computational advances in molecular spectroscopy, Ed. R. Fausto and J. M. Hollas, Kluwer Academic: The Netherlands, 1993.
- [23] Stephens, P. J. and Harada, N., ECD Cotton Effect Approximated by the Gaussian Curve and Other Methods, 2010, Chirality 22, 229-233.
- [24] Plotting UV/Vis Spectra from Oscillator & Dipole Strengths, Gaussian Tech Notes, Feb 2016. <http://gaussian.com/uvvisplot/> (Accessed March, 2017)
- [25] Ridley, J. and Zerner, M., An intermediate neglect of differential overlap technique for spectroscopy: Pyrrole and the azines, 1973, Theor. Chim. Acta, 32, 111-134.
- [26] Jacquemin D., Adamo C., Computational Molecular Electronic Spectroscopy with TD-DFT, Top Curr Chem. 2016; Vol. 368: 347-75. doi: 10.1007/128_2015_638.
- [27] Lipinski C.A., Lombardo F., Dominy B.W. and Feeney P.J., "Experimental and computational approaches to estimate solubility and permeability in drug discovery and development settings", Adv. Drug Deliv. Rev., 23, 3-25, (1997).
- [28] Kamlet, M.J., Doherty, R.M., Abboud, J.L.M., Abraham, M.H. and Taft, R.W., Linear solvation energy relationships: 36. Molecular properties governing solubilities of organic nonelectrolytes in water, 1986, J. Pharmaceutical Sci. 75, 338-349.
- [29] Mandloi M., Sikarwar A., Sapre NS., Karmarkar S. and Khadikar PV., A comparative QSAR study using Wiener, Szeged, and molecular connectivity indices, 2000, J. Chem. Inf. Comput. Sci., 40, 57-62.
- [30] Gasteiger, J. and Marsili, M., Iterative partial equalization of orbital electronegativity—a rapid access to atomic charges, 1980, Tetrahedron, 36, 3219-3228.
- [31] Stanton, D.T., Egolf, L.M., Jurs, P.C. and Hicks, M.G., Computer-assisted prediction of normal boiling points of pyrans and pyrroles, 1992, J. Chem. Inf. Comput. Sci., 32, 306-316.
- [32] Sanniraghi, A.B., Ab initio Molecular Orbital Calculations of Bond Index and Valency, 1992, Adv. Quant. Chem., 23, 301-351.
- [33] CODESSA Pro, <http://www.codessa-pro.com/descriptors/> (Accessed March, 2017).
- [34] Dragon 6, http://www.taletе.mi.it/products/dragon_molecular_descriptors.htm (Accessed March, 2017)
- [35] CORINA Symphony, <https://www.mn-am.com/products/corinasymphony> (Accessed March, 2017).
- [36] Molecular Operating Environment, https://www.chemcomp.com/MOE-Molecular_Operating_Environment.htm (Accessed March, 2017).
- [37] K. Varmuza and P. Filzmoser, Introduction to Multivariate Statistical Analysis in Chemometrics, Boca Raton, FL., CRC Press Taylor & Francis Group, 2009.
- [38] A. Gustavo González, in Chemometrics in Practical Applications, K. Varmuza, (Ed.), 2012, InTech Pub., Rijeka, Croatia, pp 19-40.
- [39] T.W. Anderson, An Introduction to Multivariate Statistical Analysis, 3rd Ed., pp. 291-458, John Wiley and Sons, New Jersey, 2003.
- [40] SPSS Statistics, <http://www-03.ibm.com/software/products/e/s/spss-statistics> (Accessed March, 2017).
- [41] Statsoft Statistica, <https://www.statsoft.com/Products/STATISTICA-Features> (Accessed March, 2017).
- [42] Fujitsu CAChe Work System Pro 7.5.0.85, 2006, http://www.fqs.pl/chemistry_materials_life_science/products/scigress (Accessed March, 2017) and Teaching with CAChe: Molecular Modeling in Chemistry, C. Wong and J. Currie, Eds., 2002, New York, Fujitsu Limited.
- [43] Miertus, S. and Tomasi, J., Approximate evaluations of the electrostatic free energy and internal energy changes in solution processes, 1982, Chem. Phys. 65, 239-245. doi:10.1016/0301-0104(82)85072-6.
- [44] Zerner, M. C., Semiempirical Molecular Orbital Methods, in Reviews in Computational Chemistry, Volume 2 (Eds. K. B. Lipkowitz and D. B. Boyd), John Wiley & Sons, Inc., Hoboken, NJ, USA, 1991. doi: 10.1002/9780470125793.ch8.
- [45] González-Arjona, D., López-Pérez, G., Domínguez, M. M. and González, A. G., Solvatochromism: A Comprehensive Project for the Final Year Undergraduate Chemistry Laboratory, 2016, J. Lab. Chem. Edu., 4(3), 45-52.
- [46] Sugiyama, K., Tsuchiya, T., Kikuchi, A. and Yagi, M., Optical and electron paramagnetic resonance studies of the excited triplet states of UV-B absorbers: 2-ethylhexyl salicylate and homomenthyl salicylate, 2015, Photochem. Photobiol. Sci., 14, 1651-1659.
- [47] Bos, J.D. and Meinardi, M.M., The 500 Dalton rule for the skin penetration of chemical compounds and drugs, 2000, Exp. Dermatol. 9, 165-169.
- [48] Abdi H. and Williams, L.J., Principal component analysis, 2010, WIREs Comp. Stat. 2, 433-459. doi: 10.1002/wics.101.
- [49] Liu, R.X., Kuang, J., Gong, Q. and Hou, X.L., Principal component regression analysis with SPSS, 2003, 71, 141-147.
- [50] Hadi A.S. and Ling, R. F., Some Cautionary Notes on the Use of Principal Components Regression, 1998, American Statistician, 52, 15-19.